

UNPICKING DATA AT THE SEAMS: VAEs, DISENTANGLEMENT AND INDEPENDENT COMPONENTS

Carl S. Allen

École Normale Supérieure, Paris
carl.allen@ens.fr

ABSTRACT

Disentanglement, or identifying salient statistically independent factors of the data, is of interest in many areas of machine learning and statistics, with relevance to synthetic data generation with controlled properties, robust classification of features, parsimonious encoding, and a greater understanding of the generative process underlying the data. Disentanglement arises in several generative paradigms, including Variational Autoencoders (VAEs), Generative Adversarial Networks and diffusion models. Particular progress has recently been made in understanding disentanglement in VAEs, where the choice of diagonal posterior covariance matrices is shown to promote mutual orthogonality between columns of the decoder’s Jacobian. We continue this thread to show how this *linear* independence translates to *statistical* independence, completing the chain in understanding how the VAE’s objective identifies independent components of, or disentangles, the data.

1 INTRODUCTION

Variational Autoencoders (VAEs, [Kingma \(2013\)](#); [Rezende et al. \(2014\)](#)) and a range of variants, e.g. β -VAE (e.g. [Higgins et al., 2017](#)) and Factor-VAE ([Kim & Mnih, 2018](#)), have been shown empirically to *disentangle* latent factors of variation in the data. For example, a trained VAE may generate face images that vary in distinct semantically meaningful ways, such as hair colour or facial expression, as individual latent variables are adjusted. This is both of practical use, e.g. for controlled generation of synthetic data with chosen properties, and intriguing as it is not knowingly designed into the training algorithm. A related phenomenon is observed in samples from a Generative Adversarial Network (GAN), which, in common with a VAE, applies a deterministic neural network function to samples of independently distributed latent variables, producing a *push-forward* distribution.

Understanding why disentanglement arises, seemingly “for free”, is of interest since identifying and separating generative factors underlying the data goes to the heart of many aspects of machine learning, from classification to generation, interpretability to identifiability, right down to a fundamental understanding of the data itself. With a better appreciation of why disentanglement happens, we might be able to induce it more reliably, particularly in domains where we cannot easily perceive when features are disentangled, as we can for images and text.

Research into the cause of disentanglement has gradually led to a refined understanding of what is meant by “disentanglement”, which typically refers to the separation of semantically meaningful generative factors ([Bengio et al., 2013](#)). Recent progress has been made towards understanding why disentanglement occurs in VAEs, tracing the root cause to the common use of *diagonal posterior covariance matrices*, a seemingly innocuous design choice made for computational efficiency ([Rolinek et al., 2019](#); [Kumar & Poole, 2020](#)). Diagonal covariances are shown to promote orthogonality between columns of the Jacobian of the decoder, a property linked to disentangled features ([Ramesh et al., 2018](#)) and independent causal mechanisms ([Gresele et al., 2021](#)). We extend this line of work by providing theoretical analysis to formally show how orthogonality in the Jacobian translates to disentanglement in the push-forward distribution of a VAE, connecting *linear* independence of partial derivatives to *statistical* independence of components, or generative factors, of the data.

Interest in understanding how disentanglement arises in VAEs has increased as their generative quality has improved (e.g. [Hazami et al., 2022](#)) and they often a key component in state of the art diffusion

models, where disentanglement is of great interest (Pandey et al., 2022; Zhang et al., 2022; Yang et al., 2023).

In this work, we pull together, analyse and extend recent advances in understanding disentanglement in VAEs. Specifically, we:

- prove that orthogonality, or *linear independence*, between columns of the encoder Jacobian corresponds to identifying *statistically independent* components of the generative distribution with distinct latent variables (§3.2);
- provide conditions under which a VAE fully identifies the data distribution (§3.2); and
- present a simple yet novel understanding of β in a β -VAE, as scaling the variance of the likelihood distribution, explaining why β affects both disentanglement and “posterior collapse” (§3.3).

2 BACKGROUND

Disentanglement: Disentanglement is not consistently defined in the literature, but typically refers to identifying salient, semantically meaningful features of the data with distinct latent variables, such that by varying a single variable, data can be generated that differ in a single aspect (Bengio et al., 2013; Higgins et al., 2017; Ramesh et al., 2018; Rolinek et al., 2019). Disentanglement has also been decomposed into necessary and sufficient-type concepts of *consistency* and *restrictiveness* (Shu et al., 2019). We show that disentanglement in a VAE relates to identifying *statistically independent components* of the data, comparable to independent component analysis (**ICA**).

Variational Autoencoder (VAE): A VAE is a latent generative model for data $x \in \mathcal{X} \doteq \mathbb{R}^m$, that models the data distribution by $p_\theta(x) = \int_z p_\theta(x|z)p(z)$ with parameters θ and latent variables $z \in \mathcal{Z} \doteq \mathbb{R}^d$. A VAE is trained by maximising a lower bound to the log likelihood (the **ELBO**),

$$\ell = \int_x p(x) \int_z q_\phi(z|x) \left\{ \log p_\theta(x|z) - \beta \log \frac{q_\phi(z|x)}{p(z)} \right\} \leq \int_x p(x) \log p_\theta(x), \quad (1)$$

where $q_\phi(z|x)$ learns to approximate the model posterior $p_\theta(z|x) \doteq \frac{p_\theta(x|z)p(z)}{p_\theta(x)}$; and $\beta = 1$. A VAE parameterises distributions by neural networks: $q_\phi(z|x) = \mathcal{N}(z; e(x), \Sigma_x)$ has mean $e(x)$ and diagonal covariance Σ_x output by an *encoder* network; and $p_\theta(x|z)$ is typically of exponential family form (e.g. Bernoulli or Gaussian) with natural parameter $\theta \doteq d(z)$ defined by a *decoder* network.¹ The prior is commonly a standard Gaussian $p(z) = \mathcal{N}(z; \mathbf{0}, \mathbf{I})$.

While samples generated from a VAE ($\beta = 1$) can exhibit disentanglement, setting $\beta > 1$ is found empirically to enhance the effect, typically with a cost to generative quality (Higgins et al., 2017).

Probabilistic Principal Component Analysis (PPCA): PPCA (Tipping & Bishop, 1999) considers a *linear* latent variable model with parameters $\mathbf{W} \in \mathbb{R}^{m \times d}$, $\sigma \in \mathbb{R}$ and noise $\epsilon \in \mathbb{R}^m$.²

$$x = \mathbf{W}z + \epsilon \quad z \sim p(z) = \mathcal{N}(z; \mathbf{0}, \mathbf{I}) \quad \epsilon \sim p_\sigma(\epsilon) = \mathcal{N}(\epsilon; \mathbf{0}, \sigma^2 \mathbf{I}), \quad (2)$$

All distributions are Gaussian and known analytically, in particular the model posterior is given by

$$p_\theta(z|x) = \mathcal{N}(z; \mathbf{M}^{-1} \mathbf{W}^\top x, \sigma^2 \mathbf{M}^{-1}) \quad \text{where} \quad \mathbf{M} = \mathbf{W}^\top \mathbf{W} + \sigma^2 \mathbf{I}. \quad (3)$$

The maximum likelihood solution is fully tractable: $\mathbf{W}_{\text{PPCA}} = \mathbf{U}(\mathbf{S} - \sigma^2 \mathbf{I})^{1/2} \mathbf{R}$, where $\mathbf{S} \in \mathbb{R}^{d \times d}$ and $\mathbf{U} \in \mathbb{R}^{m \times d}$ contain the largest eigenvalues and corresponding eigenvectors of the data covariance $\mathbf{X} \mathbf{X}^\top$, and $\mathbf{R} \in \mathbb{R}^{d \times d}$ is orthonormal ($\mathbf{R}^\top \mathbf{R} = \mathbf{I}$). As $\sigma^2 \rightarrow 0$, \mathbf{W}_{ML} approaches the singular value decomposition (**SVD**) of the data $\mathbf{X} = \mathbf{U} \mathbf{S} \mathbf{V}^\top$ up to ambiguity in \mathbf{V} , as in classical PCA. Due to the ambiguity in \mathbf{R}/\mathbf{V} , the model is considered *unidentified*. While the exact solution is known, it can also be numerically approximated by optimising the ELBO, e.g. (Eq. 1) by *expectation maximisation* (**PPCA^{EM}**), where (**E**) sets $q_\phi(z|x)$ to its exact optimum $p_\theta(z|x)$ in Eq. 3; and (**M**) optimises w.r.t. θ .

Linear VAE (LVAE): A VAE with Gaussian likelihood $p_\theta(x|z) \doteq \mathcal{N}(x; d(z), \sigma^2 \mathbf{I})$ and linear decoder $d(x) = \mathbf{W}x$ (termed a *linear* VAE assumes the same underlying model as PPCA (2). Indeed,

¹For Gaussian distributions, a fixed variance parameter σ^2 is also specified.

²We assume the data is centred since it is equivalent to including a mean parameter Tipping & Bishop (1999).

training an LVAE differs to PPCA^{EM} only in approximating the posterior by $q_\phi(z|x) = \mathcal{N}(z; \mathbf{E}x, \Sigma)$ rather than directly computing its optimum. While that may seem a backward step, [Lucas et al. \(2019\)](#) showed that the diagonal Σ of an LVAE *breaks the symmetry* of PPCA. This follows from Σ being both diagonal and optimal per Eq. 3,

$$\Sigma = \sigma^2 \mathbf{M}_{\text{PPCA}}^{-1} \doteq (\mathbf{I} + \frac{1}{\sigma^2} \mathbf{W}_{\text{PPCA}}^\top \mathbf{W}_{\text{PPCA}})^{-1} = \mathbf{R} \mathbf{S} \mathbf{R}^\top \quad \forall x, \quad (4)$$

(using the definition of \mathbf{W}_{PPCA}), which requires $\mathbf{R} = \mathbf{I}$ and restricts the solution of an LVAE to $\mathbf{W}_{\text{LVAE}} = \mathbf{U}(\mathbf{S} - \sigma^2 \mathbf{I})^{1/2}$ (cf \mathbf{W}_{PPCA}), up to trivial transformations (axis permutation and sign).

Orthogonality in a VAE Decoder’s Jacobian: Beyond symmetry breaking in *linear* VAEs, diagonal posterior covariances are shown to promote disentanglement in *non-linear* VAEs by inducing columns of the decoder’s Jacobian to be mutually orthogonal ([Rolinek et al., 2019](#); [Kumar & Poole, 2020](#)). The generalised argument of [Kumar & Poole \(2020\)](#) reparameterises around the encoder mean, $z = e(x) + \epsilon$, $\epsilon \sim \mathcal{N}(\mathbf{0}, \Sigma_x)$, and Taylor expands to approximate a *deterministic* ELBO (**det-ELBO**):

$$\begin{aligned} \ell(x) &= \mathbb{E}_{\epsilon|x} \left[\log p_\theta(x|z=e(x) + \epsilon) - \underbrace{\beta \log \frac{p(\epsilon)}{p(z=e(x)+\epsilon)}}_{\text{KL}} \right] && \text{(Reparameterise)} \\ &= \mathbb{E}_{\epsilon|x} \left[\log p_\theta(x|z=e(x)) + \epsilon^\top \mathbf{j}_{e(x)}(x) + \frac{1}{2} \epsilon^\top \mathbf{H}_{e(x)}(x) \epsilon + O(\epsilon^3) - \beta \text{KL} \right] && \text{(Taylor)} \\ &\approx \underbrace{\log p_\theta(x|z=e(x))}_{\text{AE}} + \frac{1}{2} \underbrace{\mathbf{H}_{e(x)}(x) \odot \Sigma_x}_{\text{gradient regularisation}} - \underbrace{\frac{\beta}{2} (\|e(x)\|^2 + \text{tr}(\Sigma_x))}_{\text{prior}} - \underbrace{\log |\Sigma_x| - d}_{\text{entropy}}. && (5) \end{aligned}$$

Here, $\mathbf{j}_{z^*}(x) \doteq (\frac{\partial \log p_\theta(x|z)}{\partial z_i})_i$ and $\mathbf{H}_{z^*}(x) \doteq (\frac{\partial^2 \log p_\theta(x|z)}{\partial z_i \partial z_j})_{i,j}$ are the Jacobian and Hessian of $\log p_\theta$ evaluated at $z^* \in \mathcal{Z}$; and \odot is the Frobenius (dot) product. The last step drops $\mathbb{E}_{\epsilon|x}[O(\epsilon^3)]$ terms, as [Kumar & Poole \(2020\)](#) justify (see also A.2). If $p_\theta(x|z)$ is an exponential family distribution with natural parameter defined by the encoder $\theta = d(z)$, the Hessian in Eq. 5 satisfies

$$\mathbf{H}_{e(x)}(x) = -\mathbf{D}_{e(x)}^\top \mathbf{A}_{doe(x)}^2 \mathbf{D}_{e(x)} + (x - \hat{x}_{doe(x)})^\top \mathbf{D}_{e(x)}, \quad (6)$$

where \mathbf{D}_{z^*} (\mathbf{D}_{z^*}) is the Jacobian (Hessian) of the decoder evaluated at z^* ; $\mathbf{A}_{\theta^*}^2 = -\frac{d^2}{d\theta^2} \log p_{\theta^*}(x|z) = \text{Var}[x|\theta^*]$; and $\hat{x}_{\theta^*} = \mathbb{E}[x|\theta^*]$. Note \mathbf{A}_θ is diagonal if individual dimensions x_i are conditionally independent given θ , e.g. pixel-wise noise. The last term is argued to be zero almost everywhere in common implementations, leaving $\mathbf{H}_{e(x)}(x) = -\mathbf{D}_{e(x)}^\top \mathbf{A}_{doe(x)}^2 \mathbf{D}_{e(x)}$ (see A.3 for discussion and A.4 for Gaussian and Bernoulli examples). Differentiating det-ELBO (Eq. 5) with this Hessian form reveals a connection between the decoder Jacobian \mathbf{D}_z and encoder variance Σ_x ,

$$\nabla_{\Sigma_x} \ell(x) = \frac{1}{2} (\mathbf{H}_{e(x)}(x) - \beta(\mathbf{I} - \Sigma_x^{-1})) \Rightarrow \boxed{\Sigma_x^{-1} = \mathbf{I} + \frac{1}{\beta} \mathbf{D}_{e(x)}^\top \mathbf{A}_{doe(x)}^2 \mathbf{D}_{e(x)}}. \quad (7)$$

It is argued that a diagonal Σ_x should thus drive the likelihood’s Hessian to also be diagonal, and in the Gaussian case ($\mathbf{A}_\theta = \frac{1}{\sigma} \mathbf{I}$) for columns of the decoder Jacobian $\mathbf{D}_{e(x)}$ to be *orthogonal*, $\forall x \in \mathcal{X}$.³

3 ORTHOGONALITY TO DISENTANGLEMENT

While diagonal covariances in a VAE are shown to cause orthogonality in the Jacobian (§2), the link from orthogonality to disentanglement is less clear, which we now work towards.

The SVD of any $m \times d$ matrix defines a 1-to-1 correspondence between left and right singular vectors that define orthogonal bases for \mathbb{R}^m and \mathbb{R}^d , respectively. Thus, if $\mathbf{J} = \mathbf{U} \mathbf{S} \mathbf{V}^\top$ is the SVD of a decoder’s Jacobian evaluated at $z^* \in \mathcal{Z}$, a small perturbation to z^* in the direction of $\mathbf{V}_{:,i}$ causes a small perturbation to $e(z^*)$ in $\mathbf{U}_{:,i}$. If columns of \mathbf{J} are orthogonal ($\forall z^*$), then $\mathbf{V} = \mathbf{I}$ and *all* local bases for \mathcal{Z} are the standard basis, which is therefore a global basis. Column orthogonality aside, note that if the data happens to vary in an independent factor along a path that follows the basis vectors $\mathbf{U}_{:,i}$, that factor is identifiable from the SVD of \mathbf{J} (e.g. [Ramesh et al., 2018](#)).

Note, however, that this relates two very different notions of “independence”: orthogonality, pertaining to geometric or *linear* independence; and independence of factors of a distribution, meaning *statistical*

³To lighten notation, we hereon drop subscripts and denote terms of Eq. 7 simply Σ , \mathbf{H} , \mathbf{D} , \mathbf{A} .

independence and that a distribution factorises into *independent components*. These concepts do not necessarily imply one another and it is not immediately obvious that column orthogonality in the Jacobian means that different latent dimensions correspond to statistically independent, often semantically meaningful, factors of variation in the data.

3.1 VAEs PERFORM LOCAL PCA

We briefly highlight the close relationship between the deterministic ELBO for Gaussian VAEs (A.4) and the analogue for PPCA given by the *exact* expectation of the PPCA^{EM} objective w.r.t. $q(z|x)$. To aid comparison, from Eq. 2 and 3, let $\hat{d}(z) \doteq \mathbb{E}[x|z] = \mathbf{W}z$, $\hat{e}(x) \doteq \mathbb{E}[z|x] = \mathbf{M}^{-1}\mathbf{W}^\top x$, and $\hat{\Sigma} \doteq \text{Var}[z|x] = (\mathbf{I} + \frac{1}{\sigma^2}\mathbf{W}^\top\mathbf{W})^{-1}$ (we drop constant factors and β for clarity).

$$\begin{aligned}\ell^{\text{PPCA}} &= \mathbb{E}_x \left[-\frac{1}{\sigma^2} \|x - \hat{d} \circ \hat{e}(x)\|^2 - \frac{1}{\sigma^2} (\mathbf{W}^\top\mathbf{W}) \odot \hat{\Sigma} - (\|\hat{e}(x)\|^2 + \text{tr}(\hat{\Sigma})) \right] \\ \ell^{\text{VAE}} &\approx \mathbb{E}_x \left[-\frac{1}{\sigma^2} \|x - d \circ e(x)\|^2 - \frac{1}{\sigma^2} (\mathbf{D}_{e(x)}^\top \mathbf{D}_{e(x)}) \odot \Sigma_x - (\|e(x)\|^2 + \text{tr}(\Sigma_x) - \log |\Sigma_x| - d) \right]\end{aligned}$$

The main difference lies in the second terms.⁴ In PPCA, the Hessian of the log likelihood ($-\mathbf{W}^\top\mathbf{W}$) and posterior variance ($\hat{\Sigma}$) are constant for all x , whereas in a VAE those terms are local to every $x \in \mathcal{X}$. This shows that VAEs approximately perform *local PCA* as suggested by Rolinek et al. (2019). We also see that the link between encoder covariance and the decoder Jacobian identified in Eq. 7, essentially generalises the optimal posterior covariance in linear PPCA (Tipping & Bishop, 1999):

$$\hat{\Sigma}^{\text{PPCA}} = (\mathbf{I} + \frac{1}{\sigma^2}\mathbf{W}^\top\mathbf{W})^{-1} \quad \Sigma_x^{\text{VAE}} = (\mathbf{I} + \frac{1}{\sigma^2}\mathbf{D}_{e(x)}^\top \mathbf{D}_{e(x)})^{-1}. \quad (8)$$

For later reference (§3.3), note that higher $\text{Var}[x|z] = \sigma^2$ corresponds intuitively to higher $\text{Var}[z|x] = \Sigma$ and vice versa, i.e. uncertainty in one domain goes hand in hand with uncertainty in the other.

3.2 FROM LINEAR INDEPENDENCE TO STATISTICAL INDEPENDENCE

We now develop our main result, extending prior work to explain how optimising the ELBO with diagonal posterior covariances leads to disentanglement of generative factors of the data. This elucidates how a seemingly innocuous design choice, which encourages *linear independence* between columns of the decoder’s Jacobian, disentangles *statistically independent* components of the data.

Push-forward distribution $p(\hat{x})$: The generative model of a VAE can be decomposed into stochastic and deterministic steps: sample the prior $z \sim p(z)$; apply a deterministic function $\hat{x} = \mu \circ d(z)$ (composing the decoder $d: z \mapsto \theta$ and mean function $\mu: \theta \mapsto \hat{x} \doteq \mathbb{E}[x|z]$); and add element-wise noise $x \sim p(x|\hat{x})$. In many cases, e.g. for image data, element-wise noise serves only as ‘‘blur’’ and is omitted when generating samples, hence samples come from the ‘‘push-forward’’ distribution of mean parameters $p(\hat{x})$. We consider such distributions more generally. For clarity, we define:

Definition 1 (push-forward distribution). *For a function $f: \mathcal{Z} \rightarrow \mathcal{X}$ and prior distribution $p_z(z)$ over \mathcal{Z} , the push-forward distribution $p_{f, p_z}^\#(x)$ is that defined implicitly by $\{x = f(z) \mid z \sim p_z(z)\} \subseteq \mathcal{X}$.*

Throughout, we assume:

A#1. *Latent variables are sampled from independent standard normals, $p_z(z) = \prod_{i=1}^d \mathcal{N}(z_i; 0, 1)$.*⁵

A#2. *$f: \mathcal{Z} \rightarrow \mathcal{X}$ is injective, continuous and differentiable almost everywhere (e.g. piece-wise linear).*

Under A#2, f : (i) defines $\mathcal{M}_f = \{f(z) \mid z \in \mathcal{Z}\} \subseteq \mathcal{X}$, a *quasi-differentiable* (see Appendix A.3), d -dimensional *manifold* embedded in \mathbb{R}^m supporting $p_f^\#$; (ii) is bijective between \mathcal{Z} and \mathcal{M}_f ; and (iii) by injectivity, has full-rank Jacobian \mathbf{J} (evaluated at $z^* \in \mathcal{Z}$), $\forall z^* \in \mathcal{Z}$.

Letting $\mathbf{J} = \mathbf{U}\mathbf{S}\mathbf{V}^\top$ be the SVD of \mathbf{J} ($\mathbf{U}^\top\mathbf{U} = \mathbf{I}$, $\mathbf{V}^\top\mathbf{V} = \mathbf{V}\mathbf{V}^\top = \mathbf{I}$), columns of \mathbf{V} , denoted $\mathbf{v}_i \in \mathcal{Z} \doteq \mathbb{R}^d$, define a (local) orthonormal basis for \mathcal{Z} , while columns $\mathbf{u}_i \in \mathcal{X} \doteq \mathbb{R}^m$ of \mathbf{U} define a basis for the tangent space to \mathcal{M}_f at $f(z^*)$. Let $s_i \doteq \mathbf{S}_{i,i}$ denote the i^{th} singular value. Since $\mathbf{J}\mathbf{v}_i = s_i\mathbf{u}_i$, for every $z^* \in \mathcal{Z}$ the Jacobian identifies a local basis for \mathcal{Z} with a local basis for \mathcal{X} .

⁴Note that the last two terms in ℓ^{VAE} relate only to posterior approximation so are not relevant to the comparison.

⁵Since we assume A#1 throughout, $p_z(z)$ is generally dropped from the subscript of $p_f^\#$ to lighten notation.

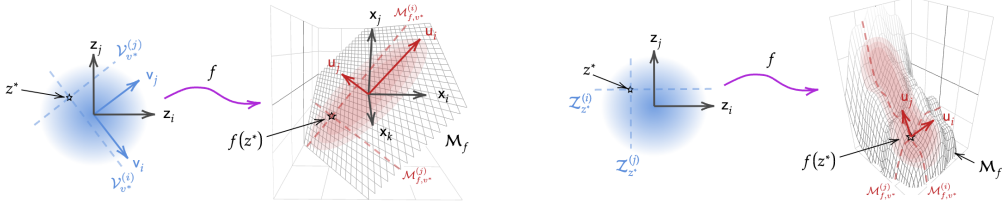


Figure 1: Translating linear independence to statistical independence: (l) **Linear f** : $z^* \in \mathcal{Z}$ is an evaluation point in the standard basis $\{z_i, z_j\}$ (denoted v^* in the V -basis $\{v_i, v_j\}$). Sub-manifolds $\mathcal{V}_{v^*}^{(i)} \subseteq \mathcal{Z}$ passing through z^* are linear, defined by varying co-ordinate i in the V -basis (dashed blue). The decoder maps $\mathcal{V}_{v^*}^{(i)}$ to linear sub-manifolds $\mathcal{M}_{f,v^*}^{(i)} \subseteq \mathcal{X}$ passing through $f(z^*)$ parallel to the U -basis (dashed red). (r) **Non-linear f , orthogonal Jacobian**: Sub-manifolds $\mathcal{Z}_{z^*}^{(i)} \subseteq \mathcal{Z}$ passing through z^* are linear, defined by varying co-ordinate i in the standard basis (dashed blue). $\mathcal{Z}_{z^*}^{(i)}$ are mapped by the decoder to sub-manifolds in \mathcal{X} that pass through $f(z^*)$ are parallel to the local U -basis (dashed red).

3.2.1 LINEAR f

For intuition, we first consider the linear model $f(z) = \mathbf{W}z$ (satisfying A#2) for which \mathcal{M}_f is a d -dimensional subspace (hyperplane through the origin), Jacobian $\mathbf{J} = \mathbf{W}$ is constant $\forall z^* \in \mathcal{Z}$, and

$$p_f^\#(x = f(z)) = |\mathbf{W}|^{-1} p(z) = \prod_i s_i^{-1} p(z_i) \quad (9)$$

factorises. We consider the factors $s_i^{-1} p(z_i)$. Let $v = \mathbf{V}^\top z$ be z expressed in the V -basis, a transformation with Jacobian $\frac{\partial v}{\partial z} = \mathbf{V}^\top$, so $p(v) = |\mathbf{V}| p(z) = p(z)$ (as expected since only the basis/perspective changes). By rotational symmetry, $p(v) = \prod_i p(v_i)$ and $p(v_i) = \mathcal{N}(0, 1)$. We can now consider x as a function of v , $x = f(z) = \mathbf{U}Sv \doteq f_V(v)$. Since $\frac{\partial x}{\partial v_i}^\top \frac{\partial x}{\partial v_j} = s_i s_j \mathbf{u}_i^\top \mathbf{u}_j = \{s_i^2 \text{ if } i=j, \text{ else } 0\}$, $(\frac{\partial x}{\partial v}) = \mathbf{U}S$ has orthogonal columns $s_i \mathbf{u}_i$ and $\|\frac{\partial x}{\partial v_i}\| = s_i$. Thus, Eq. 9 becomes

$$p_f^\#(x = f_V(v)) = \prod_i \|\frac{\partial x}{\partial v_i}\|^{-1} p(v_i), \quad (10)$$

with factors of the form of uni-variate probability distributions under a change of variables. As illustrated in Figure 1 (left), we let $v^* = \mathbf{V}^\top z^*$ denote an evaluation point in the V -basis, and define $\mathcal{V}_{v^*}^{(i)} = \{(v_1^*, \dots, v_i^*, \dots, v_d^*) \mid v_i \in \mathbb{R}\}$, that describe lines passing through v^* as each co-ordinate i (only) varies, or 1-D linear sub-manifolds of \mathcal{Z} expressed in the V -basis (blue dashed lines). Let $\mathcal{M}_{f,v^*}^{(i)} = \{f_V(v) \mid v \in \mathcal{V}_{v^*}^{(i)}\} \subseteq \mathcal{M}_f$ be the linear sub-manifold (i.e. line) traced by the image of f_V restricted to $\mathcal{V}_{v^*}^{(i)}$, essentially a single-variable function of v_i (red dashed lines). Note that for different v^* , $\mathcal{M}_{f,v^*}^{(i)}$ are always parallel to the U -basis. Each push-forward distribution $p_{f,z^*}^{\#(i)}$ for $v_i \sim p(v_i)$ and f_V restricted to $v \in \mathcal{V}_{v^*}^{(i)}$, is supported on $\mathcal{M}_{f,z^*}^{(i)}$ with density $p_{f,z^*}^{\#(i)}(x) = \|\frac{\partial x}{\partial v_i}\|^{-1} p(v_i)$, where $v = f_V^{-1}(x)$, giving meaning to the factors in Eq. 10. Thus for data points on the manifold $x \in \mathcal{M}_f$,

$$p_f^\#(x) = \prod_i p_{f,z^*}^{\#(i)}(x). \quad (11)$$

factorises as a product of distributions. Since a perturbation to $x = f(z^*) = f_V(v^*)$ in basis vector \mathbf{u}_i corresponds (exclusively) to a perturbation to v^* in v_i , only $p(v_i)$ is affected, so only $p_{f,z^*}^{\#(i)}(x)$ and no other component $p_{f,z^*}^{\#(j \neq i)}(x)$ can change. In simple terms, linearly independent basis vectors v_i in \mathcal{Z} are projected by f to linearly independent basis vectors \mathbf{u}_i in \mathcal{X} , and statistical independence over sub-manifolds defined by v_i is preserved over sub-manifolds defined by \mathbf{u}_i . In summary, this proves:

Theorem 1. Assuming A#1 (independent Gaussian latent variables) and a linear function $f : \mathcal{Z} \rightarrow \mathcal{X}$, $f(z) = \mathbf{W}z$, the push-forward distribution $p_f^\#$ factorises as a product of statistically independent components in \mathcal{X} , which align with the left singular vectors of \mathbf{W}

Remark 1. The probability density over $v \in \mathcal{V}_{v^*}^{(i)}$ is a standard Gaussian $\mathcal{N}(v; 0, 1)$. The probability density $p_{f,z^*}^{\#(i)}(x) = s_i^{-1} p(f_V^{-1}(x)_i)$ over a sub-manifold, $x \in \mathcal{M}_{f,z^*}^{(i)}$, is also Gaussian $\mathcal{N}(x; 0, s_i^2)$.

Remark 2. The SVD of the Jacobian $\mathbf{J} = \mathbf{U} \mathbf{S} \mathbf{V}^\top$ can be interpreted in terms of the chain rule $\mathbf{J} = \frac{\partial \mathbf{x}}{\partial \mathbf{u}} \frac{\partial \mathbf{u}}{\partial \mathbf{v}} \frac{\partial \mathbf{v}}{\partial \mathbf{z}}$; and as $\mathbf{U}, \mathbf{V}^\top$ transforming the basis in each domain (termed the independent bases of f), and diagonal $\mathbf{S} = \frac{\partial \mathbf{u}}{\partial \mathbf{v}}$ is the Jacobian of f for elements expressed in those independent bases. A basis vector in one domain uniquely affects one basis vector in the other: $\frac{\partial u_i}{\partial v_j} = \{s_i \text{ if } i=j; 0 \text{ o/w}\}$.

Remark 3. Since right singular vectors \mathbf{V} are a basis, or matter of perspective, they have no effect on the model and cannot be identified. Component order and direction (positive/negative sign) similarly have no effect on the data distribution.

Corollary 1.1. For data generated under the linear PPCA model (Eq. 2), an LVAE identifies statistically independent components of the data. If singular values of ground truth \mathbf{W} are distinct, the model is fully identified.

Proof. The PPCA model satisfies the assumptions of [Theorem 1](#). Columns of \mathbf{W}_{LVAE} are scalar multiples of left singular vectors of ground truth \mathbf{W} , which, by [Theorem 1](#), define statistically independent components of the data. Identifiability follows from uniqueness of $p_{f,z^*}^{\#(i)}(x)$. \square

3.2.2 NON-LINEAR f , COLUMN-ORTHOGONAL JACOBIAN

[Theorem 1](#) for linear f may be unsurprising, but notably its proof does not rely on linearity of f . We therefore follow a similar argument where f may be non-linear and we assume

A#3. $(\forall z^* \in \mathcal{Z})$ columns of \mathbf{J} are mutually orthogonal, $\frac{\partial \mathbf{x}}{\partial z_i}^\top \frac{\partial \mathbf{x}}{\partial z_j} = 0, i \neq j$; or, equivalently, $\mathbf{V} = \mathbf{I}$.

Theorem 2. Assuming [A#1-3](#), the push-forward distribution $p_f^\#$ factorises as a product of statistically independent components in \mathcal{X} and at each point z^* , those components align with columns of \mathbf{U} , the left singular vectors of the Jacobian \mathbf{J} evaluated at z^* .

Proof. The pushforward distribution satisfies

$$p_f^\#(f(z)) = |\mathbf{W}|^{-1} p(z) = \prod_i s_i^{-1} p(z_i) = \prod_i \|\frac{\partial \mathbf{x}}{\partial z_i}\|^{-1} p(z_i), \quad (12)$$

equivalent to Eq. 10 but without the need for a change of basis. As illustrated in [Figure 1 \(right\)](#) and analogously to the linear case, we define $\mathcal{Z}_{z^*}^{(i)} = \{(z_1^*, \dots, z_i, \dots, z_d^*) \mid z_i \in \mathbb{R}\}$, which describe orthogonal lines in \mathcal{Z} passing through z^* parallel to the standard basis ([blue dashed lines](#)); and uni-variate functions $f_{z^*}^{(i)}(z_i) \doteq f(z_1^*, \dots, z_i, \dots, z_d^*)$, which trace the image of f restricted to $z \in \mathcal{Z}_{z^*}^{(i)}$. By construction, each $f_{z^*}^{(i)}(z_i)$: (i) has derivative $\frac{d}{dz_i} f_{z^*}^{(i)} = \frac{\partial \mathbf{x}}{\partial z_i}$ matching a corresponding partial derivative of f ; and (ii) defines a 1-D sub-manifold $\mathcal{M}_{f,z^*}^{(i)} \doteq \{f_{z^*}^{(i)}(z_i) \mid z_i \in \mathbb{R}^d\} \subset \mathcal{M}_f$ passing through $f(z^*)$ with tangent vector $\frac{\partial \mathbf{x}}{\partial z_i}$ ([red dashed lines](#)). Since $\frac{\partial \mathbf{x}}{\partial z_i}$ are orthogonal, sub-manifolds $\mathcal{M}_{f,z^*}^{(i)}$ are orthogonal at z^* . Lastly, each tuple $\{f_{z^*}^{(i)}(z_i), z_i \sim p(z_i)\}$ defines a push-forward distribution $p_{f,z^*}^{\#(i)}(x)$ over a sub-manifold $x \in \mathcal{M}_{f,z^*}^{(i)}$, satisfying $p_{f,z^*}^{\#(i)}(x) = \|\frac{\partial \mathbf{x}}{\partial z_i}\|^{-1} p(z_i)$ for $z = f^{-1}(x)$, giving meaning to the factors of Eq. 12. Thus, for $x \in \mathcal{M}_f$,

$$p_f^\#(x) = \prod_i p_{f,z^*}^{\#(i)}(x) \quad (13)$$

factorises into uni-variate distributions supported over sub-manifolds $\mathcal{M}_{f,z^*}^{(i)}$ that are mutually orthogonal where they meet. By orthogonality, traversing sub-manifold $\mathcal{M}_{f,z^*}^{(i)}$ corresponds to varying a single latent factor z_i , hence all other probability factors remain constant and $\{\mathcal{M}_{f,z^*}^{(i)}\}_i$ serve as a (non-linear) co-ordinate system in \mathcal{X} corresponding to *statistically independent components*. \square

Remark 4. The independent basis of f is the standard basis of \mathcal{Z} and $\|\frac{\partial \mathbf{x}}{\partial z_i}\| = s_i$.

Remark 5. The probability density restricted to $z \in \mathcal{Z}_{v^*}^{(i)}$ is a standard normal Gaussian $\mathcal{N}(z; 0, 1)$. The probability density $p_{f, z^*}^{\#(i)}(x) = s_i^{-1} p(f^{-1}(x)_i)$ over $x \in \mathcal{M}_{f, z^*}^{(i)}$ is not Gaussian in general since s_i can vary over $x \in \mathcal{M}_{f, z^*}^{(i)}$.

Corollary 2.1. For data generated from a push-forward distribution $p_f^\#$, where $p(z)$ satisfies A#1 and f satisfies A#2 and A#3, a Gaussian VAE identifies statistically independent components of the data with distinct latent dimensions. If ground truth singular values s_i as a function of $z \in \mathcal{Z}_{v^*}^{(i)}$ are unique, the model is fully identified (the analogue of distinct singular values).

Proof. The data distribution and an optimised Gaussian VAE each satisfy A#1, A#2 and (from §2) A#3, so by Theorem 2, data lie on a manifold with statistically independent sub-manifolds. The VAE defines a similar manifold and its objective is maximised iff $p_\theta(x) = p(x)$, hence when distributions over VAE sub-manifolds match those over ground truth sub-manifolds. VAE sub-manifolds map 1-to-1 to latent dimensions by Theorem 2. Identifiability follows from uniqueness of $p_{f, z^*}^{\#(i)}(x)$. \square

3.2.3 NON-LINEAR f

Having seen that column orthogonality (A#3) is sufficient for independent factors in \mathcal{X} , we now consider if it is necessary. Relaxing A#3, we consider a general push-forward distribution under A#1 and A#2, i.e. independent latent variables and an injective, (quasi-)differentiable function.

In previous scenarios, sub-manifolds in $\mathcal{Z}(\mathcal{V}_{v^*}^{(i)}, \mathcal{Z}_{z^*}^{(i)})$ are linear, defined by right singular vectors of the Jacobian that are constant $\forall z \in \mathcal{Z}$. Those sub-manifolds can also be defined parametrically, as continuous paths that follow right singular vectors at each point (cf integrating over a vector field).⁶ In our relaxed scenario, singular vectors can vary $\forall z \in \mathcal{Z}$, but J is (quasi-)continuous w.r.t. z (by A#2) and the SVD of a matrix M is continuous w.r.t. M (Papadopoulou & Lourakis, 2000), hence right singular vectors v_i trace continuous sub-manifolds $\mathcal{V}^{(i)} \subseteq \mathcal{Z}$, that are orthogonal where they meet. As always for an SVD, mutually orthogonal $\mathcal{V}^{(i)} \subseteq \mathcal{Z}$ map to mutually orthogonal sub-manifolds $\mathcal{M}^{(i)} \subseteq \mathcal{X}$ and $p(x)$ factorises as a product of component push-forward distributions over each $\mathcal{M}^{(i)}$. However, sub-manifolds $\mathcal{V}^{(i)} \subseteq \mathcal{Z}$ need not be linear and are not necessarily statistically independent, i.e. the density at $z^* \in \mathcal{Z}$ may not equal the product of densities over $\mathcal{V}^{(i)} \subseteq \mathcal{Z}$ passing through z^* .

This suggests that either: (1) sub-manifolds are not statistically independent and $p(x)$ can not necessarily factorise as a product of independent components, i.e. f entangles z_i ; or (2) sub-manifolds are statistically independent and map under f to independent factors in \mathcal{X} . In case 2, since an optimal Gaussian VAE maps independent components $\mathcal{M}^{(i)} \subseteq \mathcal{X}$ to the standard basis in \mathcal{Z} , independent factors in \mathcal{X} can be identified, but sub-manifolds $\mathcal{V}^{(i)} \subseteq \mathcal{Z}$ are unidentifiable, analogous to V in PCA.

3.3 INTERPRETING β OF β -VAE

Note that β in Eq. 1 has played no role, yet is seen to affect disentanglement (Higgins et al., 2017), we therefore consider its role in the (β) -ELBO. Previous works interpret β as re-weighting the KL and reconstruction components of the ELBO, or serving as a Lagrange multiplier for a KL ‘constraint’. We provide an interpretation more in keeping with the original ELBO.

To model data from a given domain, a (β) -VAE requires a suitable likelihood $p_\theta(x|z)$, e.g. a Gaussian likelihood for coloured images, and a Bernoulli for black and white images where pixel values $x^k \in [0, 1]$ are bounded (Higgins et al., 2017). In the Gaussian case, dividing Eq. 1 by β shows that training a β -VAE with encoder variance $\text{Var}[x|z] = \sigma^2$ is equivalent to a VAE with $\text{Var}[x|z] = \beta\sigma^2$ and adjusted learning rate (Lucas et al., 2019). We now interpret β for other likelihoods.

In the Bernoulli example mentioned above, black and white image pixels are not strictly black or white ($x^k \in \{0, 1\}$) and may lie between ($x^k \in [0, 1]$), hence the Bernoulli distribution appears invalid as it does not sum to 1 over the domain of x^k . That is, unless each sample is treated as the mean \bar{x} of multiple (true) Bernoulli samples. Multiplying the likelihood by a factor $\kappa > 1$ is then tantamount to scaling the number of observations as though each were made κ times, lowering the variance of the

⁶e.g. $v^{(i)}(t) \in \mathcal{V}_{v^*}^{(i)}$, $v^{(i)}(t) = v^* + \int_0^t \frac{dv}{dt} dt = v^* + t\mathbf{v}_i$ (where $\frac{dv}{dt} = \frac{\partial v_i}{\partial z}(v(t)) = \mathbf{v}_i$)

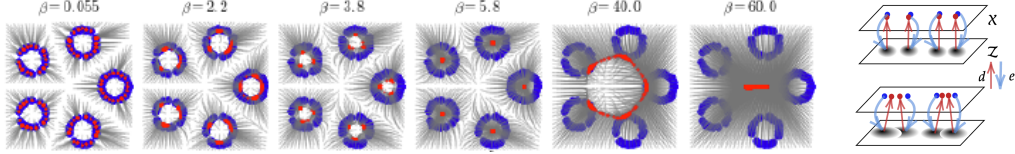


Figure 2: Effect of $\text{Var}[x|z]$, or β , on reconstruction (blue = data, red = reconstruction): (l) For low β ($\beta = 0.55$), $\text{Var}[x|z]$ is low, by Eq. 7 & 8, and data are closely reconstructed (see right, top). As β increases, $\text{Var}[x|z]$ and so $\text{Var}[z|x]$ increase and posteriors of nearby data points $\{x_i\}$ increasingly overlap (see right, bottom). For z in overlap of $\{q(z|x_i)\}$, the decoder $\mathbb{E}[x|z]$ maps to a weighted average of $\{x_i\}$. Initially, close neighbours map to their mean ($\beta = 2.2, 3.8$), then small circles “become neighbours” and map to their centroids, until finally all samples map to the global centroid ($\beta = 60$). (reproduced with permission from [Rezende & Viola, 2018](#)) (r) illustrating posterior overlap, (t) low β , (b) higher β .

“mean” observation, $\text{Var}[\bar{x}] \xrightarrow{\kappa \rightarrow \infty} 0$.⁷ Thus, multiplying the KL term by β in a β -VAE, or equivalently dividing the likelihood by β , amounts to scaling the likelihood’s variance by β , just as in the Gaussian case: **higher β** corresponds to lower κ (“fewer observations”) and so **higher likelihood variance**. Since the argument holds for any exponential family likelihood, we have proved

Theorem 3 (β -VAE $_{\sigma^2} \equiv$ VAE $_{\beta\sigma^2}$). *If the likelihood $p_\theta(x|z)$ is of exponential family form, a β -VAE with $\text{Var}[x|z] = \sigma^2$ is equivalent to a VAE with $\text{Var}[x|z] = \beta\sigma^2$.*

In the most general case, the β -ELBO (Eq. 1) is maximised if $q(z|x) \propto p_\theta(x|z)^{1/\beta} p(z)$, and β can be interpreted as a *temperature* parameter: high β dilates the likelihood towards a uniform distribution (high $\text{Var}[x|z]$), low β concentrates it towards a delta distribution (low $\text{Var}[x|z]$).

Figure 2, from [Rezende & Viola \(2018\)](#), nicely illustrates the effect of varying β and empirically demonstrates the relationship to $\text{Var}[x|z]$. As variance increases, posteriors of nearby data points $\{x_i\}$ (blue) increasingly overlap (by Eq. 7/8) and the decoder maps latents in regions of overlap to weighted averages of x_i (red). Since $\text{Var}[x|z]$ governs how close data points need to be for this effect, it acts as a “glue” over $x \in \mathcal{X}$ (see caption for details). This justifies why increasing β enhances connections in latent space for nearby, likely semantically related, data ([Higgins et al., 2017](#)).

We note that Theorem 3 also allows clearer interpretation of other works that vary β . While setting $\beta > 1$ can enhance disentanglement, setting $\beta < 1$ is found to mitigate “posterior collapse” (**PC**), which describes when a VAE’s likelihood is sufficiently expressive such that it learns to directly model the data distribution, $p(x|z) = p(x)$, leaving latent variables redundant ([Bowman et al., 2015](#)).

Corollary 3.1 ($\beta < 1$). *Setting $\beta < 1$ is expected to mitigate posterior collapse.*

Proof. From Theorem 3, $\beta < 1$ reduces $\text{Var}[x|z]$, constraining the distributional family that $p_\theta(x|z)$ can describe. For some β , $\text{Var}[x|z] < \text{Var}[x]$ and so $p(x) \neq p_\theta(x|z)$, $\forall \theta$, making PC impossible. \square

4 REVISITING THE PROOF OF JACOBIAN ORTHOGONALITY

Having established that orthogonality in the Jacobian is key to disentangling independent components, we go back and (i) *prove* that a diagonal covariance matrix Σ_x leads to a diagonal Hessian, and (ii) consider the optimal singular values of the decoder Jacobian.

Theorem 4. *[Diagonal Hessian] det-ELBO (Eq. 5) is maximised w.r.t. eigenvectors \mathbf{V}_H of \mathbf{H} iff $\mathbf{V}_H = \mathbf{I}$, $\forall x$.*

See [Appendix B](#) for a proof (by the Cauchy-Schwartz inequality with matrix trace norm) and as a sanity check, a proof that the optimum holds when considering Σ as a function of \mathbf{H} , i.e. assuming

A#4. *The decoder is sufficiently optimised to maintain the relationship in Eq. 7: $\Sigma = (\mathbf{I} - \frac{1}{\beta} \mathbf{H})^{-1}$.*

This confirms the hypothesis of [Kumar & Poole \(2020\)](#) that the det-ELBO is maximised if \mathbf{H} is diagonal ([§2](#)). We note that \mathbf{H} and its eigenvectors \mathbf{V} are not parameters that are directly optimised. Neither are typically computed and both can vary for every x . Rather, Theorem 4 indicates implicit pressure during optimisation, as [Rolinek et al. \(2019\)](#) and [Kumar & Poole \(2020\)](#) verify empirically.

⁷A mode-parameterised Beta distribution could also be considered, but we keep to a more general argument.

Optimal S : Jacobian components U and S serve very different purposes. For a trained VAE, the singular vectors U track the manifold on which $p(x)$ is supported and must pass close to observed data points, i.e. reconstruct them. Meanwhile, singular values s_i determine (i) the rate at which the manifold is traversed along u_i relative to a change to z^* by v_i , and reciprocally (ii) how density “spreads” over the manifold: loosely speaking, larger $s_i = \frac{\partial v_i}{\partial u_i}$ implies more rapid traversal and so transported density is spread more thinly.

For a Gaussian likelihood, we assume optimal values $\Sigma_x = \text{diag}[\mathbf{I} - \frac{1}{\beta} \mathbf{H}]^{-1}$ (by Eq. 7) and $\mathbf{V}_H = \mathbf{I}$ (by Theorem 4) are maintained. Omitting factors that do not affect optimisation, Eq. 5 becomes:

$$\ell = \mathbb{E} \left[-\|x - d\phi(e(x))\|^2 - S^2(\mathbf{I} + \frac{1}{\beta} S^2)^{-1} - \beta \|e(x)\|^2 \right], \quad (14)$$

where $\mathbf{J} = \mathbf{U}S$ is the SVD of the decoder Jacobian (since $\mathbf{V} = \mathbf{I}$). If the encoder is sufficiently flexible that its value is independent of its Jacobian (unlike a linear function, say), Eq. 14 suggests that S and U are optimised by different terms: the first (reconstruction) term trains U to fit observed data points, the second term trains S . We consider the optimal S .

The second term $-S^2(\mathbf{I} + \frac{1}{\beta} S^2)^{-1} \in (-\beta \mathbf{I}, \mathbf{0})$ decreases monotonically with components of S , hence the ELBO is maximised if $S \rightarrow \mathbf{0}$ wherever evaluated, i.e. at data points. As $s_i \doteq \frac{du_i}{dv_i} \rightarrow 0$, the decoder becomes (locally) stationary, maximising the likelihood $p(x) = |\frac{dx}{dz}|^{-1} p(z) \rightarrow \infty$. However, assuming we observe at least two distinct data points $x^{(1)} \neq x^{(2)} \in \mathcal{X}$ (with co-ordinates $u^{(1)}, u^{(2)}$ in the U -basis, mapped by the decoder from $v^{(1)}, v^{(2)}$ in the V -basis), then s_i cannot be zero everywhere or the manifold cannot be traversed from $x^{(1)}$ to $x^{(2)}$, i.e. the data cannot be reconstructed. Treating u as a function of v , a VAE maximises $-(\frac{du}{dv})^2(\mathbf{I} + \frac{1}{\beta}(\frac{du}{dv})^2)^{-1}$, subject to $\int_{v^{(1)}}^{v^{(2)}} \frac{du}{dv} dv = u^{(2)} - u^{(1)}$. This is a calculus of variations problem, but it is immediate that the VAE objective is maximised if $u(v)$ passes through $x^{(1)}$ and $x^{(2)}$ with zero gradient everywhere except at sharp jumps between “plateaus”. (In the limit, jumps are discontinuous with measure zero, but we assume d is continuous.)

Thus, the VAE objective promotes over-fitting to observed data (or memorisation), which is mitigated in practice by, for example, training on more data, using a decoder family that is *not* a universal approximator, or regularising the decoder to impose a Lipschitz-type constraint. Nevertheless, optimising S encourages density on the VAE’s manifold to concentrate around observed data points and, by Eq. 7, for posterior covariances to tend to the covariance of the prior, $\Sigma_x \rightarrow \mathbf{I}$.

5 RELATED WORK

Many works study aspects or variants of VAEs, or disentanglement in other modelling paradigms. Here, we review those that offer insight into understanding the underlying cause of disentanglement in VAEs. Higgins et al. (2017) first showed that disentanglement is enhanced by increasing β in Eq. 1, and Burgess et al. (2018) hypothesised that diagonal posterior covariances may be the cause, encouraging latent dimensions to align with generative factors of the data. Rolinek et al. (2019) showed theoretically and empirically that diagonal posterior covariances promote orthogonality in the decoder’s Jacobian, which they deemed responsible for disentanglement. Kumar & Poole (2020) simplified and generalised that argument. These works demonstrated that diagonal posteriors provide an inductive bias that breaks the rotational symmetry of an isometric Gaussian prior, side-stepping impossibility results related to independent component analysis (e.g. Locatello et al., 2019). Several works investigate the more analytically tractable objective and learning dynamics of linear VAEs (Lucas et al., 2019; Bao et al., 2020; Koehler et al., 2022). Zietlow et al. (2021) show that disentanglement is sensitive to perturbations to the data distribution. Reizinger et al. (2022) relate the VAE objective to *independent causal mechanisms* (Gresele et al., 2021) which consider *non-statistically independent* sources that contribute to a mixing function by orthogonal columns of the Jacobian. This clearly relates to the orthogonal Jacobian bias of VAEs, but differs to our approach that identifies statistically independent components/sources. Ramesh et al. (2018) trace independent factors by following leading left singular vectors of the Jacobian of a GAN generator. In the opposite direction, Chadebec & Allassonnière (2022) trace manifolds in latent space by following a locally averaged metric derived from VAE posterior co-variances. Pan et al. (2023) claim that the data manifold is identifiable from a geometric perspective assuming Jacobian-orthogonality, which

differs to our focus on statistical independence. More recently, [Bhowal et al. \(2024\)](#) consider the encoder/decoder dissected into linear and non-linear aspects, loosely resembling our view of the Jacobian in terms of linear bases from its SVD. However, the decoder function is quite different to its Jacobian and dissecting a function into linear and non-linear components is not well defined whereas an SVD is unique.

6 CONCLUSION

Unsupervised disentanglement of independent factors of the data is a fundamental aim of machine learning and significant recent progress has been made in the case of VAEs. We extend that work to show that the choice of diagonal posterior covariances in a VAE causes statistically independent components of the data to align with distinct latent variables of the model, i.e. disentanglement. In the process, we provide a novel yet straightforward interpretation of β in a β -VAE, which plausibly explains why increasing β promotes disentanglement but degrades generation quality; while decreasing β mitigates posterior collapse. We also supplement the proof of orthogonality by showing that the likelihood's Hessian is necessarily encouraged to be diagonal and giving a detailed analysis of the Jacobian's optimal singular values.

Neural networks are often considered too complex to explain, yet recent advances make their deployment in everyday applications all but inevitable. Improved theoretical understanding is therefore essential to be able to confidently take full advantage of machine learning progress, possibly in critical systems, and we hope that the body of work that we add to here is a useful step. Interestingly, our approach rests on the fact that, regardless of the model's complexity, its Jacobian, which transforms the density of the prior, can be considered in relatively simple terms.

Not only is a better understanding of VAEs of interest in itself, VAEs are often part of the pipeline in recent diffusion models that achieve state-of-the-art generative performance (e.g. [Pandey et al., 2022](#); [Yang et al., 2023](#); [Zhang et al., 2022](#)). Other recent works show that supervised learning ([Dhuliawala et al., 2023](#)) and self-supervised learning ([Bizeul et al., 2024](#)) can be viewed from a latent variable perspective and trained under a suitable variant of the ELBO, connecting VAEs to other learning paradigms in a common mathematical language.

One limitation of our work and of current understanding more generally is that disentanglement is observed in VAEs with non-Gaussian likelihoods ([Higgins et al., 2017](#)), whereas current work, including ours, only explains the Gaussian case. We plan to address this in future work.

REFERENCES

Xuchan Bao, James Lucas, Sushant Sachdeva, and Roger B Grosse. Regularized linear autoencoders recover the principal components, eventually. In *NeurIPS*, 2020.

Yoshua Bengio, Aaron Courville, and Pascal Vincent. Representation learning: A review and new perspectives. *IEEE transactions on pattern analysis and machine intelligence*, 35(8):1798–1828, 2013.

Pratik Bhowal, Achint Soni, and Sirisha Rambhatla. Why do variational autoencoders really promote disentanglement? In *ICML*, 2024.

Alice Bizeul, Bernhard Schölkopf, and Carl Allen. A probabilistic model to explain self-supervised representation learning. *arXiv preprint arXiv:2402.01399*, 2024.

Samuel R Bowman, Luke Vilnis, Oriol Vinyals, Andrew M Dai, Rafal Jozefowicz, and Samy Bengio. Generating sentences from a continuous space. *arXiv preprint arXiv:1511.06349*, 2015.

Christopher P Burgess, Irina Higgins, Arka Pal, Loic Matthey, Nick Watters, Guillaume Desjardins, and Alexander Lerchner. Understanding disentangling in β -vae. *arXiv preprint arXiv:1804.03599*, 2018.

Clément Chadebec and Stéphanie Allassonnière. A geometric perspective on variational autoencoders. In *NeurIPS*, 2022.

Shehzaad Dhuliawala, Mrinmaya Sachan, and Carl Allen. Variational classification. *TMLR*, 2023.

Luigi Gresele, Julius Von Kügelgen, Vincent Stimper, Bernhard Schölkopf, and Michel Besserve. Independent mechanism analysis, a new concept? In *NeurIPS*, 2021.

Louay Hazami, Rayhane Mama, and Ragavan Thurairatnam. Efficientvdvae: Less is more. *arXiv preprint arXiv:2203.13751*, 2022.

Irina Higgins, Loic Matthey, Arka Pal, Christopher Burgess, Xavier Glorot, Matthew Botvinick, Shakir Mohamed, and Alexander Lerchner. β -VAE: Learning Basic Visual Concepts with a Constrained Variational Framework. In *ICLR*, 2017.

Hyunjik Kim and Andriy Mnih. Disentangling by factorising. In *ICML*, 2018.

Diederik P Kingma. Auto-encoding variational bayes. *arXiv preprint arXiv:1312.6114*, 2013.

Frederic Koehler, Viraj Mehta, Chenghui Zhou, and Andrej Risteski. Variational autoencoders in the presence of low-dimensional data: landscape and implicit bias. In *ICLR*, 2022.

Abhishek Kumar and Ben Poole. On Implicit Regularization in β -VAEs. In *ICML*, 2020.

Francesco Locatello, Stefan Bauer, Mario Lucic, Gunnar Raetsch, Sylvain Gelly, Bernhard Schölkopf, and Olivier Bachem. Challenging common assumptions in the unsupervised learning of disentangled representations. In *ICML*, 2019.

James Lucas, George Tucker, Roger B Grosse, and Mohammad Norouzi. Don't Blame the ELBO! a Linear VAE Perspective on Posterior Collapse. In *NeurIPS*, 2019.

Ziqi Pan, Li Niu, and Liqing Zhang. Geometric inductive biases for identifiable unsupervised learning of disentangled representations. In *AAAI*, 2023.

Kushagra Pandey, Avideep Mukherjee, Piyush Rai, and Abhishek Kumar. Diffusevae: Efficient, controllable and high-fidelity generation from low-dimensional latents. *Transactions on Machine Learning Research*, 2022.

Théodore Papadopoulos and Manolis IA Lourakis. Estimating the jacobian of the singular value decomposition: Theory and applications. In *ECCV*, 2000.

Aditya Ramesh, Youngduck Choi, and Yann LeCun. A spectral regularizer for unsupervised disentanglement. *arXiv preprint arXiv:1812.01161*, 2018.

Patrik Reizinger, Luigi Gresele, Jack Brady, Julius Von Kügelgen, Dominik Zietlow, Bernhard Schölkopf, Georg Martius, Wieland Brendel, and Michel Besserve. Embrace the gap: Vaes perform independent mechanism analysis. In *NeurIPS*, 2022.

Danilo Jimenez Rezende and Fabio Viola. Taming vaes. *arXiv preprint arXiv:1810.00597*, 2018.

Danilo Jimenez Rezende, Shakir Mohamed, and Daan Wierstra. Stochastic backpropagation and approximate inference in deep generative models. In *International conference on machine learning*, pp. 1278–1286. PMLR, 2014.

Michal Rolinek, Dominik Zietlow, and Georg Martius. Variational Autoencoders Pursue PCA Directions (by Accident). In *CVPR*, 2019.

Rui Shu, Yining Chen, Abhishek Kumar, Stefano Ermon, and Ben Poole. Weakly supervised disentanglement with guarantees. In *ICLR*, 2019.

Michael E Tipping and Christopher M Bishop. Probabilistic principal component analysis. *Journal of the Royal Statistical Society Series B: Statistical Methodology*, 61(3):611–622, 1999.

Tao Yang, Yuwang Wang, Yan Lu, and Nanning Zheng. Disdiff: unsupervised disentanglement of diffusion probabilistic models. In *NeurIPS*, 2023.

Zijian Zhang, Zhou Zhao, and Zhijie Lin. Unsupervised representation learning from pre-trained diffusion probabilistic models. *NeurIPS*, 2022.

Dominik Zietlow, Michal Rolinek, and Georg Martius. Demystifying inductive biases for (beta-) vae based architectures. In *ICML*, 2021.

A APPENDIX: DIAGONAL COVARIANCE \Rightarrow JACOBIAN ORTHOGONALITY

A.1 DERIVATION OF DETERMINISTIC ELBO

The steps in the derivation of Eq. 5 by [Kumar & Poole \(2020\)](#) can be summarised as follows:

$$\begin{aligned}
 \ell(x) &= \mathbb{E}_{\epsilon|x} \left[\log p_\theta(x|z=e(x) + \epsilon) - \underbrace{\beta \log \frac{p(\epsilon)}{p(z=e(x)+\epsilon)}}_{\text{KL}} \right] && \text{(Reparameterise)} \\
 &= \mathbb{E}_{\epsilon|x} \left[\log p_\theta(x|z=e(x)) + \epsilon^\top \mathbf{j}_{e(x)}(x) + \frac{1}{2} \epsilon^\top \mathbf{H}_{e(x)}(x) \epsilon + O(\epsilon^3) - \beta \text{KL} \right] && \text{(Taylor)} \\
 &\approx \underbrace{\log p_\theta(x|z=e(x))}_{\text{AE}} + \underbrace{\frac{1}{2} \mathbf{H}_{e(x)}(x) \odot \Sigma_x}_{\text{gradient regularisation}} - \underbrace{\frac{\beta}{2} (\|e(x)\|^2 + \text{tr}(\Sigma_x))}_{\text{prior}} - \underbrace{\log |\Sigma_x| - d}_{\text{entropy}}, && (15)
 \end{aligned}$$

where $\mathbf{j}_{z^*}(x) \doteq (\frac{\partial \log p_\theta(x|z)}{\partial z_i})_i$ and $\mathbf{H}_{z^*}(x) \doteq (\frac{\partial^2 \log p_\theta(x|z)}{\partial z_i \partial z_j})_{i,j}$ are the Jacobian and Hessian of p_θ evaluated at z^* ; and \odot is the Frobenius (dot) product.

A.2 ON THE ACCURACY OF THE TAYLOR SERIES APPROXIMATION

In support of the validity of the Taylor approximation in Eq. 5, we note that:

1. expectations of odd powers vanish by symmetry of $p(\epsilon)$, so the approximation is 4th-order;
2. the first term in Eq. 5 is maximised if $\hat{x}_{e(x)} \doteq \eta' \circ d(e(x)) = x$, i.e. each mean *reconstructs* the data, hence the second term in Eq. 6 vanishes as reconstruction improves;
3. accurate reconstructions require posteriors to not significantly overlap ?, hence as the number of data samples increases, posterior variances must decrease to avoid overlap and higher order Taylor series terms decrease exponentially; and
4. it may be possible to choose activation functions with fewer higher-order derivatives (see [Appendix A.3](#)).

A.3 COMPATIBILITY OF PIECE-WISE LINEAR FUNCTIONS WITH TAYLOR APPROXIMATION

In §2, the proof that maximising the VAE objective (Eq. 5) promotes orthogonality in the decoder's Jacobian assumes that the log-likelihood is well approximated by its Taylor series. For a decoder with piece-wise linear activation functions $f \in \mathcal{C}^0$, e.g. commonly used (leaky-)ReLU, the log-likelihood is non-differentiable at finitely many points, around which it diverges from its Taylor series, weakening the approximation in Eq. 5. However, the proof is valid if f can be approximated arbitrarily well by a differentiable $g_\tau \in \mathcal{C}^1$ with $\lim_{\tau \rightarrow \infty} g_\tau = f$, e.g. $\text{ReLU}(x) \doteq \max(0, x) = \lim_{\tau \rightarrow \infty} \frac{1}{\tau} \log(1 + e^{\tau x})$. We can then consider f replaced by g_τ (with arbitrarily large τ) such that abrupt changes in derivative of f are accounted for by the Taylor series rather than omitted (see [Kumar & Poole, 2020](#), eq. 5).

We note that the spirit of the argument in [Kumar & Poole \(2020\)](#) is maintained if g^τ can be chosen to have few higher order components. Further, the terms that the authors suggest can be omitted vanish in any case as training of the VAE progresses (see [Appendix A.2](#), point 2).

We consider the manifold $\{e(z)|z \in \mathcal{Z}\} \subset \mathcal{X}$ associated with a \mathcal{C}^0 decoder as **quasi-differentiable** from a similar limiting argument.

A.4 DETERMINISTIC ELBO OBJECTIVE FOR SPECIFIC EXPONENTIAL FAMILY LIKELIHOODS

For commonly used Gaussian and Bernoulli likelihoods, the deterministic ELBO Eq. 5 is given by

$$\ell(x) \approx \begin{cases} -\frac{1}{2\sigma^2} \|x - d \circ e(x)\|^2 - \frac{1}{2\sigma^2} (\mathbf{D}_{e(x)}^\top \mathbf{D}_{e(x)}) \odot \Sigma_x - \beta \text{KL} & \text{(Gaussian)} \\ x^\top \log s(d \circ e(x)) - \frac{1}{2} (\mathbf{D}_{e(x)}^\top \mathbf{B}_{d \circ e(x)} \mathbf{D}_{e(x)}) \odot \Sigma_x - \beta \text{KL} & \text{(Bernoulli)} \end{cases}$$

where $s(\theta)$ is the (element-wise) logistic sigmoid and \mathbf{B}_θ is a diagonal matrix of Bernoulli variances $s(\theta_i)(1-s(\theta_i))$ evaluated at $\theta = d \circ e(x)$.

B APPENDIX: OPTIMAL EIGENVALUES OF THE HESSIAN

Theorem 4. [Diagonal Hessian] *det-ELBO (Eq. 5) is maximised w.r.t. eigenvectors \mathbf{V}_H of \mathbf{H} iff $\mathbf{V}_H = \mathbf{I}$, $\forall x$.*

[back to [Theorem 4](#)]

Proof. (We drop subscripts x to ease notation). Let $\mathbf{V}\mathbf{T}\mathbf{V}^\top$ be the eigen-decomposition of \mathbf{H} . We want to maximise w.r.t. \mathbf{V} , the deterministic ELBO

$$\ell(x) = \log p_\theta(x|z=e(x)) + \frac{1}{2}\mathbf{H} \odot \Sigma - \frac{\beta}{2}(\|e(x)\|^2 + \text{tr}(\Sigma) - \log |\Sigma| - d), \quad (16)$$

hence we want to maximise $\mathbf{H} \odot \Sigma$. Since Σ is diagonal, the problem can be stated as

$$\max_{\mathbf{V}} \mathbf{H} \odot \Sigma = \text{tr}(\mathbf{H}\Sigma) = \text{tr}(\mathbf{V}\mathbf{T}\mathbf{V}^\top \Sigma) = \text{tr}((\mathbf{V}\mathbf{T})(\Sigma\mathbf{V})^\top) \doteq \langle \mathbf{V}\mathbf{T}, \Sigma\mathbf{V} \rangle, \quad (17)$$

where $\langle \mathbf{A}, \mathbf{B} \rangle \doteq \text{tr}(\mathbf{A}, \mathbf{B}^\top)$ defines an inner product over matrices with implied norm $\|\mathbf{A}\| \doteq \langle \mathbf{A}, \mathbf{B} \rangle^{1/2}$ (it is straightforward to confirm $\langle \cdot, \cdot \rangle$ satisfies the necessary axioms). By the Cauchy-Schwartz inequality:

$$\begin{aligned} \mathbf{H} \odot \Sigma &= \langle \mathbf{V}\mathbf{T}, \Sigma\mathbf{V} \rangle \leq \|\mathbf{V}\mathbf{T}\| \|\Sigma\mathbf{V}\| = \text{tr}(\mathbf{V}\mathbf{T}^2\mathbf{V}^\top)^{1/2} \text{tr}(\Sigma\mathbf{V}\mathbf{V}^\top\Sigma)^{1/2} \\ &= \text{tr}(\mathbf{T}^2\mathbf{V}^\top\mathbf{V})^{1/2} \text{tr}(\Sigma\mathbf{V}\mathbf{V}^\top\Sigma)^{1/2} \\ &= \text{tr}(\mathbf{T}^2)^{1/2} \text{tr}(\Sigma^2)^{1/2} = \mathbf{T} \odot \Sigma \end{aligned} \quad (18)$$

where we have used $\mathbf{V}^\top\mathbf{V} = \mathbf{V}\mathbf{V}^\top = \mathbf{I}$ since $\mathbf{H} \doteq \text{Var}[x|z=e(x)]$ is symmetric.

Thus the deterministic ELBO is maximised iff $\mathbf{V} = \mathbf{I}$, $\forall x$. \square

Since Σ is known to depend on \mathbf{H} , we verify the above result by considering the optimal \mathbf{V} when Σ “keeps up” with \mathbf{H} , i.e.

A#4. *The decoder is sufficiently optimised to maintain the relationship in Eq. 7: $\Sigma = (\mathbf{I} - \frac{1}{\beta}\mathbf{H})^{-1}$.*

Theorem 5. *Under A#4, the deterministic ELBO (Eq. 5) is maximised w.r.t the eigenvectors $\mathbf{V}_H \in \mathbb{R}^{d \times d}$ of \mathbf{H} iff $\mathbf{V}_H = \mathbf{I}$, $\forall x$.*

Proof. (We drop subscripts x to ease notation) By Eq. 7 (valid for all covariance matrices) and A#4, $\Sigma^{-1} = \mathbf{I} - \frac{1}{\beta}\mathbf{H}$. For diagonal Σ of interest, we have $\Sigma = \text{diag}[\mathbf{I} - \frac{1}{\beta}\mathbf{H}]^{-1}$, where $\text{diag}[\mathbf{M}]$ zeros out all but the diagonal elements of \mathbf{M} . (We note that $\text{diag}[\mathbf{M}]^{-1} \neq \text{diag}[\mathbf{M}^{-1}]$, in general.)

Since $\mathbf{H} \doteq \text{Var}[x|z=e(x)]$ is symmetric, $\mathbf{V}^\top\mathbf{V} = \mathbf{V}\mathbf{V}^\top = \mathbf{I}$. Let $\mathbf{v}_i \in \mathbb{R}^d$ be row i of \mathbf{V} and consider each term $\ell(x)$ of the deterministic ELBO (Eq. 5):

$$\begin{aligned} \ell(x) &= \underbrace{\log p_\theta(x|e(x)) - \frac{\beta}{2}\|e(x)\|^2 + \frac{\beta d}{2}}_c + \frac{1}{2}\mathbf{H} \odot \Sigma - \frac{\beta}{2}(\text{tr}(\Sigma) - \log |\Sigma|) \\ &= c + \frac{\beta d}{2} - \frac{\beta}{2} \sum_i (-\frac{1}{\beta}\mathbf{v}_i^\top \mathbf{T} \mathbf{v}_i)(1 - \frac{1}{\beta}\mathbf{v}_i^\top \mathbf{T} \mathbf{v}_i)^{-1} + (1 - \frac{1}{\beta}\mathbf{v}_i^\top \mathbf{T} \mathbf{v}_i)^{-1} + \log(1 - \frac{1}{\beta}\mathbf{v}_i^\top \mathbf{T} \mathbf{v}_i) \\ &= c - \frac{\beta}{2} \sum_i \log(1 - \frac{1}{\beta}\mathbf{v}_i^\top \mathbf{T} \mathbf{v}_i) \\ &= c - \beta \log \prod_i \|(\mathbf{I} - \frac{1}{\beta}\mathbf{T})^{1/2} \mathbf{v}_i\| \\ &\leq c - \beta \log |(\mathbf{I} - \frac{1}{\beta}\mathbf{T})^{1/2} \mathbf{V}| \quad (\text{Hadamard's inequality}) \\ &= c - \beta \log \prod_i \|(\mathbf{I} - \frac{1}{\beta}\mathbf{T})^{1/2}\| \end{aligned} \quad (19)$$

Comparing Eq. 19 to the last line, we see that the ELBO (Eq. 5) is maximised w.r.t. \mathbf{V}_H iff $\mathbf{V}_H = \mathbf{I}$. \square